KSCE Journal of Civil Engineering
DOI 10.1007/s12205-024-2637-4

pISSN 1226-7988, eISSN 1976-3808
www.springer.com/12205

Tunnel Engineering

Research on Mechanical Characteristics and Failure Mechanism of Coal-Rock Combined Bodies with Equal Strength

Maolin Tian[a], **Anfu Zhang**[a], **Dawei Yin**[b], **Hongtian Xiao**[c], **Lijun Han**[d], **and Zishuo Liu**[d]

[a]*Shandong Key Laboratory of Civil Engineering Disaster Prevention and Mitigation, Shandong University of Science and Technology, Qingdao 266590, China*
[b]*College of Energy and Mining Engineering, Shandong University of Science and Technology, Qingdao 266590, China*
[c]*College of Civil Engineering and Architecture, Shandong University of Science and Technology, Qingdao 266590, China*
[d]*State Key Laboratory of Intelligent Construction and Healthy Operation and Maintenance of Deep Underground Engineering, China University of Mining and Technology, Xuzhou 221116, China*

ARTICLE HISTORY

Received 13 December 2023
Revised 31 March 2024
Accepted 9 May 2024
Published Online 6 July 2024

KEYWORDS

Similar materials
Coal-rock combination
Uniaxial compression test
Mechanical property
Failure mechanism

ABSTRACT

To investigate the distortion and damage properties of coal-rock combination (CRC) samples, the individual coal samples and rock samples and CRC were developed by similar materials with equal strength. Then, uniaxial compression (UC) tests and acoustic emission (AE) tests were performed on CRC samples with various rock-coal height ratios and loading rates. The strength, deformation, and AE properties of the CRC samples were analyzed to explore their failure mechanisms. The findings indicated that the individual coal samples and rock samples were mainly damaged by tensile splitting. For CRC samples, shear and tensile coupled failures were the main failure modes. Cracks are first generated from coal part and continue to expand to rock part. The coal-rock height ratio had little impact on the single AE event count peak value but had a certain influence on the cumulative number of AE event count. However, the loading rate had a large effect on the AE characteristics, and the strength and elastic modulus (E) of the CRC samples had linear or nonlinear increasing trend with increasing ratio of rock to coal height and loading rate. The research findings will have certain theoretical reference value for analyzing the mechanism of coal pillar failure.

1. Introduction

At the time of coal mining, not only is the body of coal itself often broken, but the adjacent rock mass is damaged, resulting in overall destabilization and failure of the coal-rock mixed seam. Therefore, the importance of studying the mechanical characteristics and injure mechanisms of coal-rock combination (CRC) is self-evident.

The mechanical properties and damage modes of CRC are an important basis for studying affect among coal seams and surrounding rock, as well as their effect on mining safety and surrounding rock stability. Therefore, numerous experimental studies have been conducted by experts and scholars to explore the mechanical properties and damage behavior of CRC, including uniaxial compression (UC) tests and cyclic loading tests (Okubo et al., 2006; Chen et al., 2018; Gong et al., 2018; Chakraborty et al., 2019; Dambly et al., 2019; Závacký and Štefaňák, 2019; Wang et al., 2020; Das et al., 2021; Ma et al., 2021; Choi et al., 2022; Wang et al., 2022a; Abi et al., 2023; Fan et al., 2024b). Furthermore, Li et al. (2020) conducted research on prepared briquette, mortar and their combination, specifically analyzing the crushing degree and energy absorption properties of coal and rock components in the CRC. They concluded that rock components had an inhibiting effect on the radial deformation of coal components. Yin et al. (2021) and Gao et al. (2020) explored the damage mode and energy variation of CRC during UC tests. Yang et al. (2022) employed UC testing to research the effect of coal thickness on the strength and damage mode of CRC samples. Li et al. (2022) employed UC testing to investigate the characteristics of disparate combinations of sequential twin material combination. Xu et al. (2023) conducted the properties and characteristics of rock spalling through compression tests, revealed that the formation process of rock spalling was influenced by both inclination angle and the number

CORRESPONDENCE Hongtian Xiao xiaohongtian@tsinghua.org.cn College of Civil Engineering and Architecture, Shandong University of Science and Technology, Qingdao 266590, China

of defects. Xiong et al. (2023) employed UC tests to investigate the cracking and strain changes of coal specimens, thereby obtained predictive information on the damage of coal specimens. Li et al. (2021) employed relevant theories to analyze the microseismic and electromagnetic radiation properties of coal-rock during evolution of rockburst, elucidating relationship between energy accumulation and dissipation, as well as the micro- and macro-scale properties of CRC specimens. Their study provides a foundation for predicting rockbursts by explaining their underlying causes. Zhang (2019) investigated the precursor of coal and rock failure by means of acoustic emission and infrared thermography tests. Tan et al. (2017, 2018) used laboratory tests to investigate the response of CRC samples to impacts and identified rock strength and height ratio as factors that influenced their behavior. Bai et al. (2019) tried to investigate damage mechanism of samples of disparate types of interbedded CRC. Liu et al. (2018) s explored the mechanical properties of coal in CRC samples by developing an equation for damaged and fitting it to data, yielding findings were consistent with expectations. Xia et al. (2021) and Zhang et al. (2021) explored the implication of coal inclination angle on the strength properties of CRC, revealing that as the angle of inclination increases it leads to larger damage values and less strain. Yang et al. (2021) explored the mathematical model of multi-field coupling in the cyclic loading process of CRC. Wang et al. (2020a) and Fan et al. (2024a) investigated the sensitivity of disparate CRC with nonuniform characteristics to blasting tendency. Ma et al. (2022a) investigated the characteristics of strength distortion, acoustic emission (AE) and failure of CRC samples with various fracture angles under UC. Yang et al. (2020) studied the influences of disparate rock-coal proportions on the damage characteristics of CRC samples by UC tests. Zhao et al. (2021) investigated the influence of rock strength on the damage evolution of CRC samples through ultrasonic and UC tests.

Most of the above experts and scholars have carried out experimental research on coal-rock combination samples by on-site sampling. Additionally, mechanical properties and failure mechanisms of CRC has been studied in increasing depth. After conducting laboratory tests and field monitoring, researchers have performed in-depth studies on the fracture modes, intensity, and distortion characteristics of CRC. Corresponding theoretical models and numerical simulation methods have been established. Based on the verification of the material model, Ma et al. (2022b) used LS-DYNA explicit dynamics software to study stress wave propagation, deformation and failure during dynamic splitting of CRC specimens under disparate impact loads, impact directions and loading angles. Wang and Tian (2018) and Zhang et al. (2020) employed numerical simulation software to investigate the failure and instability characteristics of CRC samples, and to analyze crack propagation within CRC samples. Khazaei et al. (2015), Shadrin and Klishin (2018) and Ali et al. (2023) explored the damage properties of coal, and a statistical model of damage during coal failure was established by AE tests. Wang et al. (2022b) proposed a pre-cracking macroscopic elastic model applicable to different forms of CRC samples, quantitatively describing the connection between the mechanical characteristics of the coal rock matrix and the pre-crack macroscopic deformation of the sample, and determining the model parameters according to the axial crack evolution characteristics. Through numerical simulation, Yin et al. (2018) and Chen et al. (2019) investigated the effect of the joint inclination angle, rock-coal height ratio in coal, and loading rate on the various characteristics of CRC specimens. Based on the test results, Wang and Ma (2022) proposed a constitutive model of strain soften the damage of assemblages and a methodology to solve for values of model arguments. They also discussed the effect of the model arguments on the constitutive model.

Many experts and scholars have studied the mechanical characteristics and failure behavior of CRC, which has great significance as guidance for safe operation of coal mines. However, many test samples are collected on-site. Although CRC structures are commonly found in actual projects, it is difficult to collect samples on-site due to complex working conditions. The obtained CRC samples have large individual differences and cannot be repeatedly tested. It takes considerable manpower and time to prepare samples in the laboratory, and it is not convenient to analyze the test results for research purposes. Therefore, this study used materials of equal strength to prepare individual coal and rock samples as well as CRC. The mechanical response of the composites under uniaxial loading conditions was investigated, with a focus on analyzing their mechanical characteristics, failure modes, and mechanism for different height ratios and loading rates. The results of this research provide a theoretical foundation for exploring the distortion behavior and support of CRC strata.

2. Preparation of CRC Specimens with Equal Strength

2.1 Selection of Materials

Considering the difficulty of on-site sampling, in this study, individual of coal samples and rock samples with equal strength materials were developed according to laboratory test requirements to replace standard samples, and CRC samples were prepared for studies deformation, failure characteristics and damage evolution of CRC samples. The preparation of materials with equal strength was as follows:

First, the rock type replaced in this paper was mudstone, which was characterized as grayish black in the upper part, dark gray in the lower part, thick layer, broken as a whole and easy to weather. In combination with the requirements of sample size and equal strength, selection of quartz sand as aggregates for coal samples with equal strength materials and chosen ordinary Portland cement and gypsum as bonding materials. The rock sample also used quartz sand as the main aggregate. Additionally, iron powder was added in an appropriate amount to meet the bulk density requirements to increase the weight. The cementing materials were aluminate cement and gypsum.

Second, to develop materials more reasonably and conveniently with equal strength, such as coal and rock that met the requirements, the orthogonal design method was used to design the ratio test.

Table 1. Factors and Levels of Materials in Individual Coal and Rock Samples with Equal Strength

Level	Ratios of materials in samples with equal strength of coal			Ratios of materials in samples with equal strength of rock		
	Paste-mud ratio	Sand-binder ratio	Water-binder ratio	Sand-binder ratio	Iron-binder ratio	Water-binder ratio
1	0.25	1.2	0.7	0.8	0.10	0.3
2	0.43	1.4	0.8	1.0	0.15	0.4
3	0.67	1.6	0.9	1.2	0.20	0.5

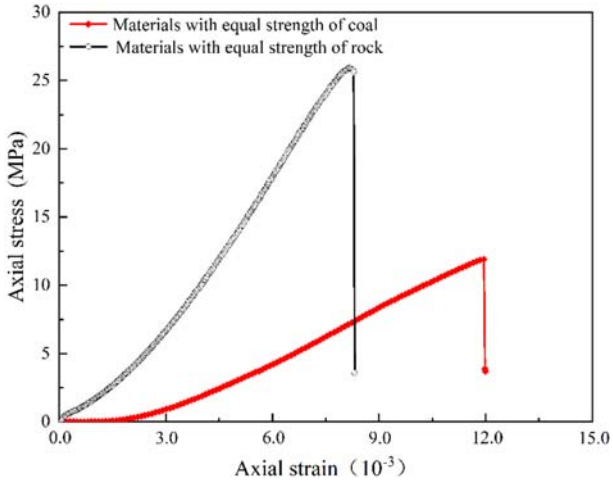

Fig. 1. σ-ε Curves of Materials with Equal Strength of Coal and Rock

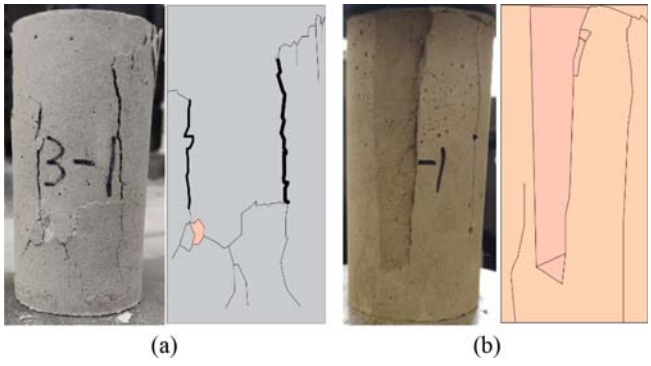

Fig. 2. Typical Failure Characteristics of Coal and Rock Samples with Equal Strength: (a) Coal, (b) Rock

According to the test requirements, the $L_9(3^4)$ orthogonal design table was selected for the experimental design of the proportion of rock, coal, and other materials. The factors and levels of materials in individual rock and coal samples with equal strength are indicated in Table 1.

Finally, individual samples of coal and rock with equal strength materials were poured and maintained according to the mix ratio shown in Table 1. Three samples were poured for each group, and the average value of uniaxial tests data for the three samples was taken as the elastic modulus (E), UC strength, and so forth of group. A microcomputer-controlled electronic universal testing machine was utilized to operate the uniaxial test, with displacement loading control way, and a loading speed of 0.002 mm/s was employed. The stress-strain (σ-ε) curves and typical damage characteristics of some specimens are shown in Figs. 1 and 2.

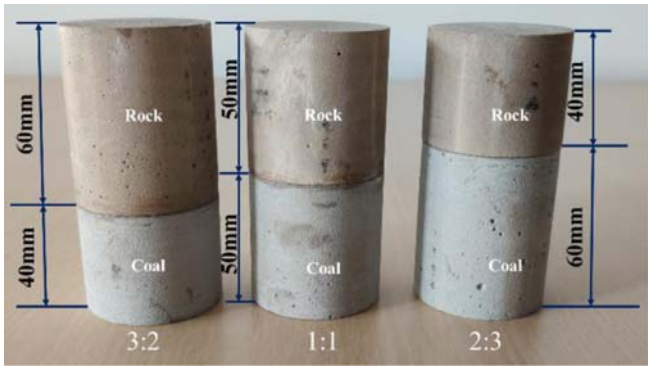

Fig. 3. Some Examples of CRC with Equal Strength

According to the test results, the ratio scheme for coal and rock materials with equal strength were selected to prepare coal and rock samples with equal strength.

2.2 Preparation of Samples of CRC with Equal Strength

To achieve a well-homogenized CRC sample, the first step was to pour a cuboid composite CRC sample with dimensions of 500 mm (length) × 500 mm (width) × 220 mm (height). The lower layer consisted of equal strength materials of coal with a height of 110 mm, while the upper layer was composed of equal strength materials of rock with a height of 110 mm. To reduce the influencing factors of the failure of the CRC, bond the combination samples together from top to bottom with a strong adhesive. The adhesive should be coated as thin as possible and ensure uniformity. The cuboid CRC sample was obtained by stirring, vibrating, and demolding.

Obtain a 220 mm-thick cuboid CRC specimen by pouring, curing, and so forth, and then drilling, cutting, and grinding processes were used to obtain each cylindrical CRC sample (100 mm × 50 mm) that met the requirements. According to the requirements for standard samples, CRC was produced with rock-coal height ratios of 2:3, 1:1, and 3:2. Some examples of CRC samples were indicated in Fig. 3.

For the convenience of description, the following rules are used for sample numbering: Taking R2C3-4a as an example, R represents rock samples with equal strength and C represents coal samples with equal strength. The digit 2 after R represents the height ratio of rock samples with equal strength and the digit 3 after C represents the height ratio of coal samples with equal strength. The number 4 after the short bar corresponds to the loading rate of 0.004 mm/s, and the letter a represents the first sample under this condition. Similarly, taking R-6-1 as an

example, R represents rock samples with equal strength and the number 6 after the short bar corresponds to the loading rate of 0.006 mm/s, and the digit 1 represents the first sample under this condition.

3. Test System and Methodology

The test system selected for this test included: a DDL-500 electronic universal testing machine, a static strain testing system, and an AE monitoring system, as shown in Fig. 4. In this test, the AE monitoring system used a PCI-II full-information AE signal analyzer from American Acoustics Corporation to monitor the AE activity of the sample during the test. The sampling frequency of the probe was set to 1 MHz. Adhesive tape was used to fix the AE probe, and the coupling agent, vaseline, was evenly applied on the link surface between the specimen and the probe to reduce attenuation of the AE signal and enhance the value of AE monitoring. Two strain gauges, one placed horizontally and the other vertically, which were affixed symmetrically to the rock and coal components of a composite specimen for monitoring the axial and radial strains of both components during loading, as depicted in Fig. 5.

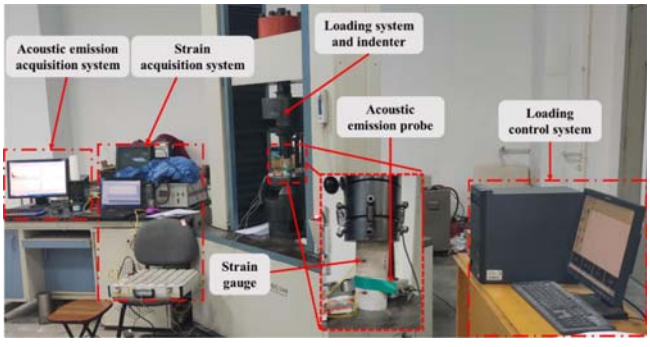

Fig. 4. Experimental System for Loading, AE Measurement and Strain Measurement

UC tests of CRC were conducted for disparate loading rates and rock-coal height ratios. The mechanical responses of CRC with equal strength were evaluated uniaxial loading conditions. The test schemes mainly included the following two parts:

1. UC test of individual coal and rock samples with equal strength under different loading rates
   The test employed standard cylindrical samples with dimensions of Φ50 × 100 mm, the loading rates were 0.002 mm/s, 0.004 mm/s and 0.006 mm/s respectively, and the displacement control loading way was used for the test.
2. UC test of CRC samples with equal strength for disparate coal-rock height ratios and loading rates
   The diameter and total height of each CRC were 50 mm and 100 mm, respectively, and three kinds of rock-coal height ratio samples of 2:3, 1:1 and 3:2 were selected to perform the test. The displacement-controlled loading way was employed in the test, with loading rates of 0.002 mm/s, 0.004 mm/s and 0.006 mm/s.

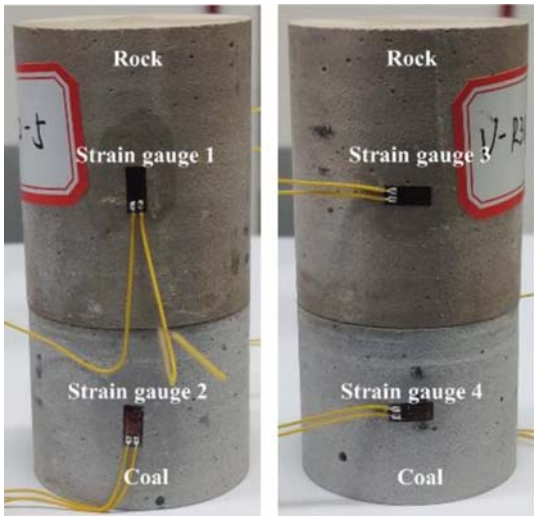

Fig. 5. Strain Gauge Locations

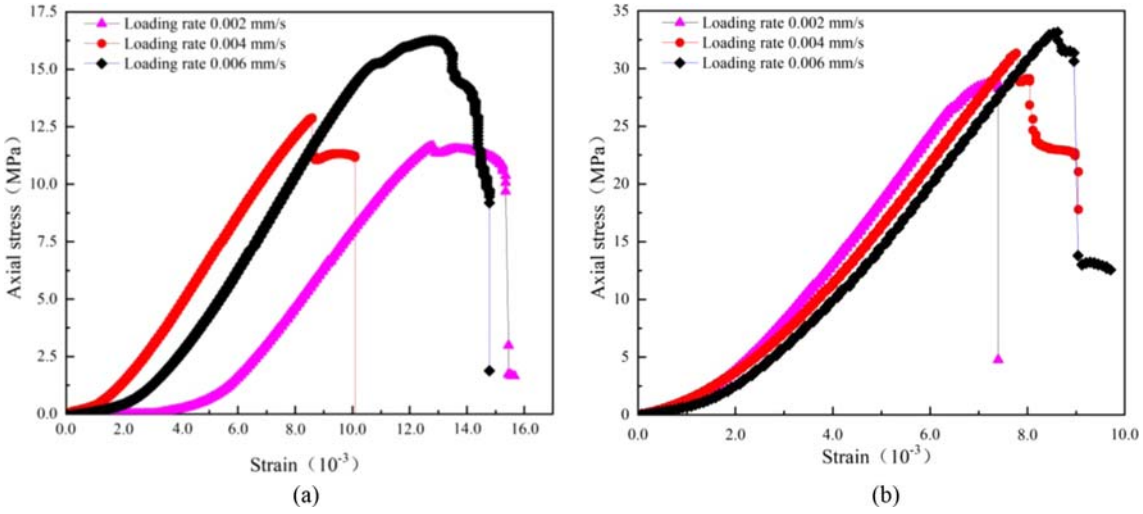

Fig. 6. σ-ε Curves of Single Specimens with Equal Strength of Coal and Rock: (a) Single Specimens of Coal, (b) Single Specimens of Rock

4. Analysis of Test Results

4.1 Intensity Characteristics

4.1.1 Intensity Characteristics of Individual Coal and Rock Specimens

Figure 6 shows the σ-ε curves of the individual samples with equal strength of coal rock at disparate loading rates. For every sample, there was an obvious drop property after the peak, and the σ-ε curve showed four stages: compaction, elastic distortion, plastic yield, and post-peak damage. The compaction stage was more obvious for individual samples with equal strength of coal, and the deformation at this stage was significantly larger than that of individual samples with equal strength of rock, while the post-peak brittle failure of individual samples with of rock was more obvious. Some samples of coal underwent a short strain softening stage after the peak.

The scatter diagram in Fig. 7 illustrates the axial peak strength of single coal and rock samples with equal strength at disparate loading rates.

In Fig. 7, the peak intensities of single samples of coal and rock increased with increasing loading rate. The average peak strengths of samples of coal increased by 9.62% and 32.43%, and the strengths of samples of rock increased by 7.40% and 14.31%, with increasing loading rate. The peak strengths of the rock samples increased linearly with increasing loading rate, while those of the coal samples increased nonlinearly. In addition, by comparing the average strength of the two samples in the ratio scheme, the strength of both samples was improved. This was because the ratio scheme was poured with a cylindrical mold, and there was uneven vibration in the pouring process. In the later stage, the equal strength samples were made by pouring cuboid first and then cutting and grinding. In the pouring process, the vibrating rod was used to vibrate evenly. The interior of the sample was denser and the pores were relatively few. Therefore, the strength was slightly higher than that of the ratio scheme.

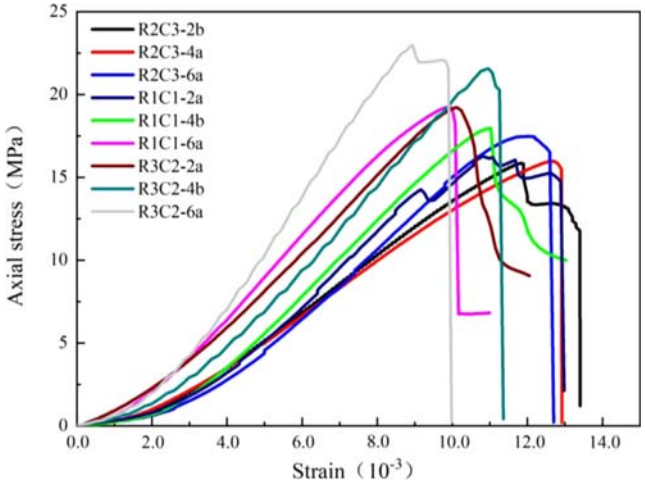

Fig. 8. UC σ-ε Curves of CRC Sample

4.1.2 Strength Properties of CRC

Figure 8 shows the UC σ-ε curves of CRC samples disparate height ratios and loading rates. The curves of all samples were basically consistent. Except for a few samples that showed obvious post-peak softening, the rest of the CRC samples showed an obvious brittle drop after the peak, and the curves also had four stages. When the loading rate was fast, the microcracks of the sample did not fully develop, and in the loading process, crack development was in the main failure surface. When the loading rate was slows, multiple microcracks developed and there was enough time for the sample to adjust its bearing structure to carry the axial load. As a result, the curves fluctuated.

To better analyze the connection between the coal-rock height ratio and loading rate for the CRC samples with equal strength, the correlations between the ratio of rock-coal height and strength and the loading rate and strength were analyzed, and the results were fitted linearly. The results for the linear fits are shown in Fig. 9.

Figure 9(a) indicated that the strength of the CRC samples increased with increasing coal-rock height ratio. This was due to

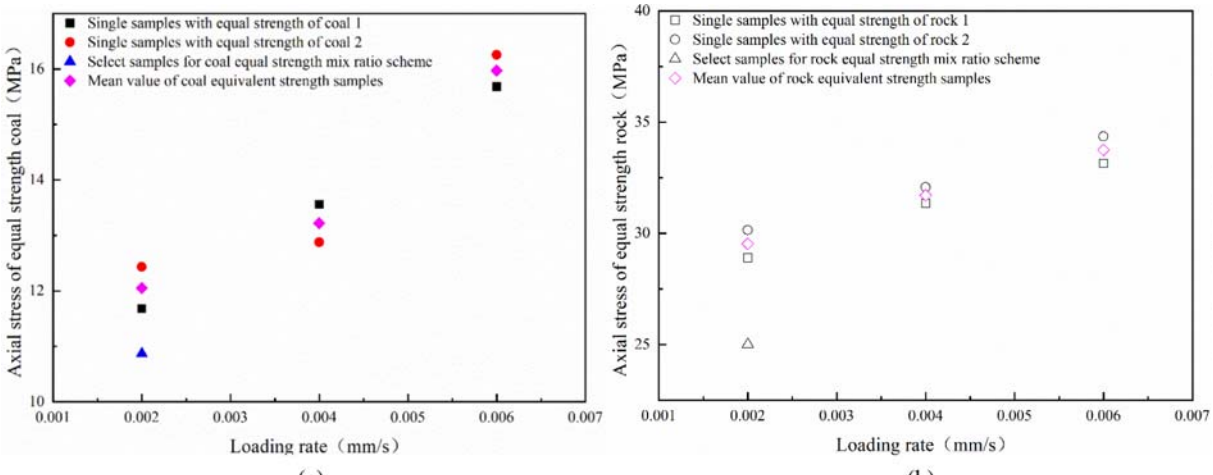

Fig. 7. Scatter Diagram of Peak Strength of Single Coal and Rock Samples with Equal Strength: (a) Coal, (b) Rock

the high strength of part of the rock specimen. The distortion was small for the rock specimen than the coal sample. Additionally, the ring effect (clamping friction) formed between the rock specimen and the coal specimen at the coal-rock interface, which played a certain role in limiting the distortion of the coal specimen and increased carrying capacity of the CRC sample to certain

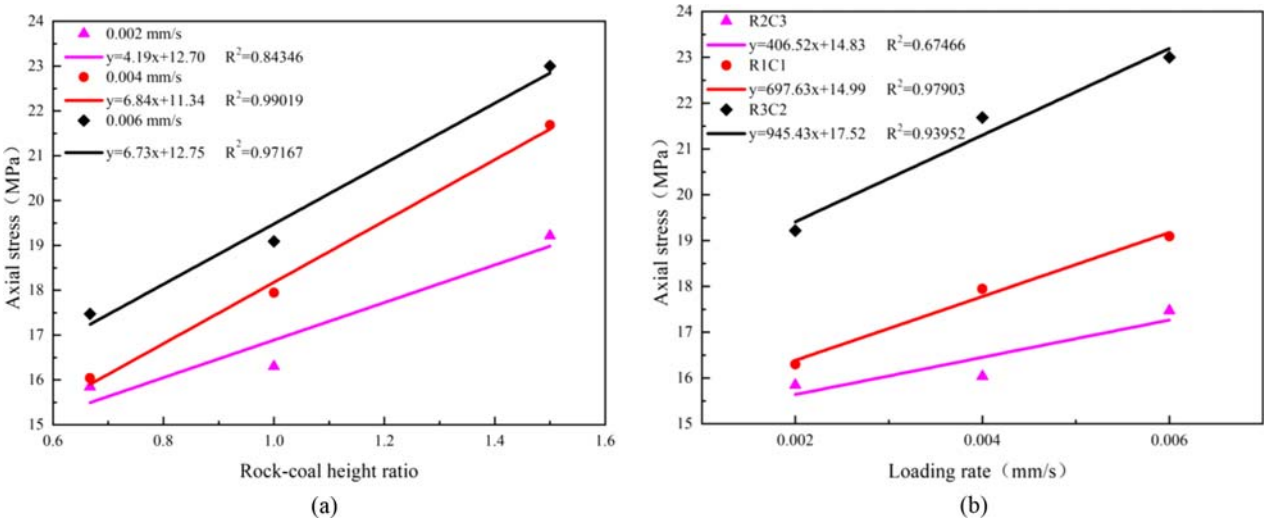

Fig. 9. Strength Evolution of CRC Samples: (a) Strength Varies with Rock-Coal Height Ratio, (b) Strength Varies with Loading Rate

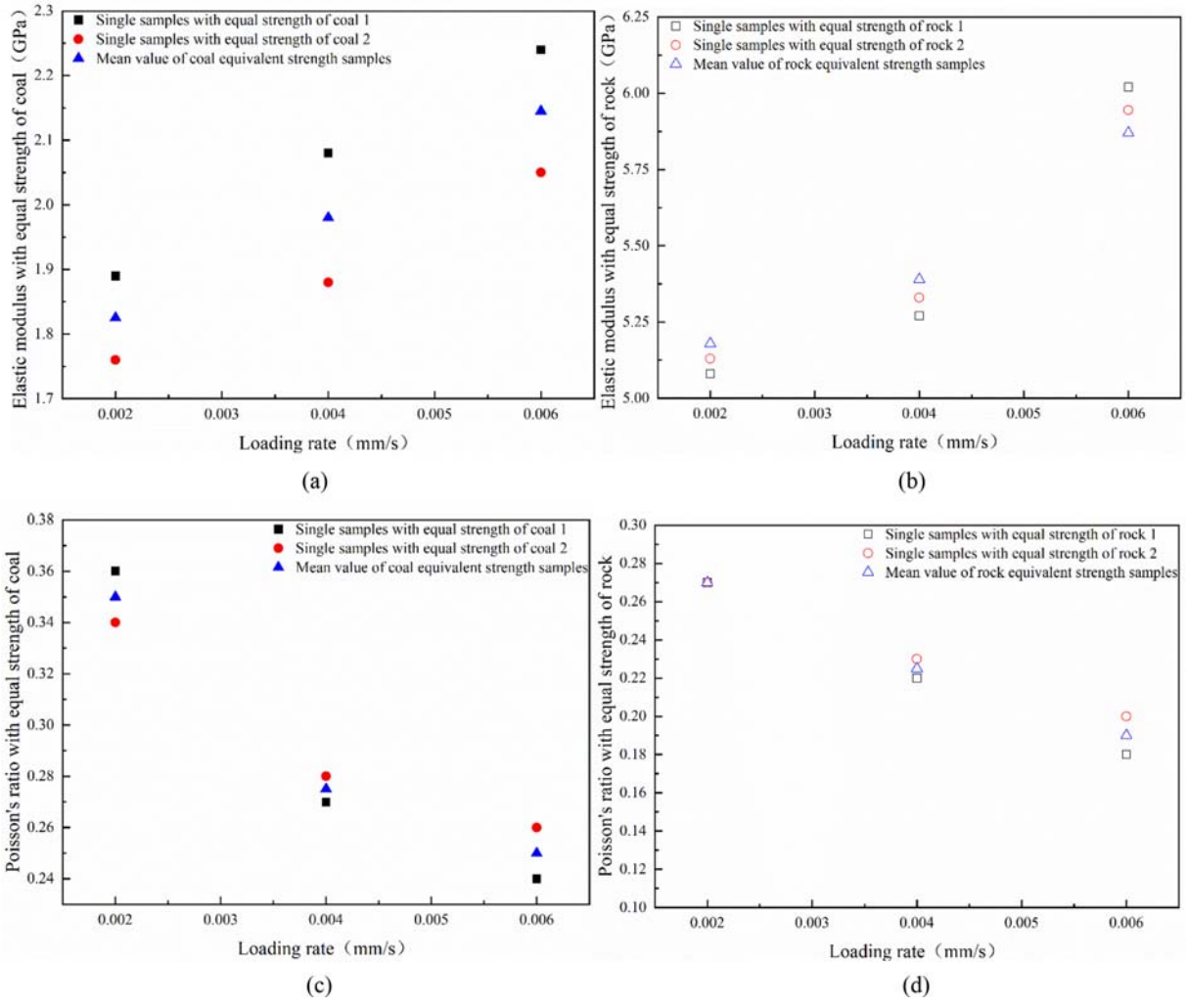

Fig. 10. Scatter Diagrams of E and μ of Individual Samples with Equal Strength of Coal and Rock: (a) Coal-E, (b) Rock-E, (c) Coal-μ, (d) Rock-μ

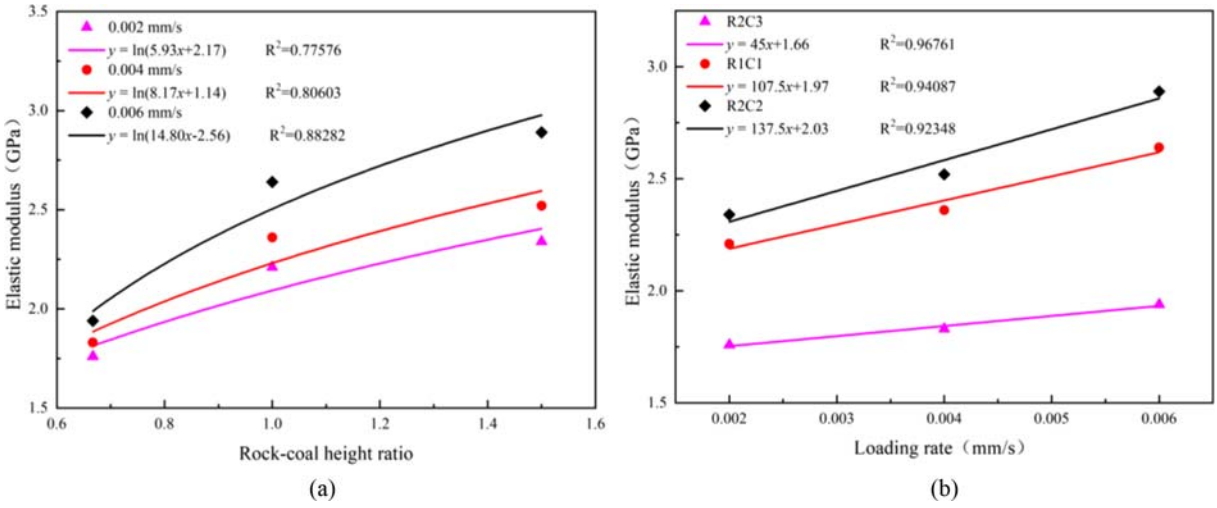

Fig. 11. *E* Evolution of CRC Samples: (a) *E* Varies with Rock-Coal Height Ratio, (b) *E* Varies with the Loading Rate

extent. When the loading rate was fast (0.004 or 0.006 mm/s), the correlation coefficients were 0.99019 and 0.97167, respectively, indicating a strong linear correlation between the strength and the ratio of rock-coal height. When the loading rate was slow (0.002 mm/s), the correlation coefficient was less than 0.84346, indicating that the linear correlation between the two was weaker with slow loading rates. Fig. 9(b) shows that the strength faster with increasing loading rate, which was generally correspond the implication of the loading rate on samples with equal strength of coal and rock. When the rock-coal height was relatively large (1:1 and 3:2), the correlation coefficient of the strength and loading rate was greater than 0.80 which showed a strong linear correlation. When the height ratio of rock and coal was small (2:3), the correlation coefficient between strength and loading rate was 0.67466, which was much less than 0.80, indicating that the linear correlation between the two was weak, and a linear relationship was not obvious.

4.2 Deformation Properties

4.2.1 Deformation Properties of Individual Coal and Rock Specimens

The slope at the peak strength of 40% – 60% of the curve was selected as *E* of specimen. Combined with the radial strain of the specimen tested by the strain monitoring system, Poisson's ratio (μ) of the specimen was obtained. Fig. 10 shows scatter diagrams of the μ and *E* of individual samples of coal and rock at different loading rates.

As shown in Fig. 10, under different loading speeds, the modulus of elasticity was significantly for the sample of coal than the sample of rock, but value of μ was large, indicating the sample of coal had little resistance to external deformation. In addition, as the loading rate increases, the *E* of two groups increased to varying degrees, while μ decreased to varying degrees. The average *E* of the coal sample increased by 8.49% and 17.53%, respectively, while that of the rock sample increased by 3.75% and 15.89%.

4.2.2 Deformation Properties of CRC Specimens

4.2.2.1 Elastic Modulus

A Similar, the correlation analysis was conducted on the connection between the *E* and coal-rock height ratio, as well as the loading rate and the *E*, and the results were fitted accordingly. The fitted results were shown in Fig. 11.

Figure 11(a) showed that the *E* of the CRC increased with increasing coal-rock height ratio. This was explained by same reason that the strength increases with coal-rock height ratio, although relationship between coal-rock height ratio and *E* was a nonlinear function rather than a linear relationship. As the loading speed was fast (0.004 and 0.006 mm/s), all the correlation coefficients were greater than 0.80, indicating that the selected logarithmic function provided a good fit for connection between coal-rock height ratio and *E*. As the loading speed was 0.002 mm/s, the correlation coefficient was less than 0.80, indicating that selected logarithmic function provided a poor fit to the relationship under the condition of the slow loading rate. Fig. 11(b) shows that the *E* increased with rising loading speed and showed a strong linear correlation, which was consistent with the effect of loading speed on coal samples. The lesser the coal-rock height ratio was, the better the linear fit. This was mainly because for the CRC sample, partial deformation of coal was the main effect, and the greater the height ratio of the coal specimen was, the closer the *E* of the CRC sample to the coal specimen, and smaller fluctuations of the *E*.

4.2.2.2 Strain Analysis

For each CRC, the axial deformation was the sum of the axial distortion of the rock sample and coal sample, that is:

$$\Delta h_{rm} = \Delta h_r + \Delta h_m \ . \tag{1}$$

In the formula, Δh_{rm}, Δh_r and Δh_m are the axial distortion of the combination, rock, and coal, separately. The axial strain of the CRC sample and the strain in rock and coal samples can be

Table 2. UC Test Results of CRC under Disparate Height Ratios and Loading Rates

Loading rate (mm/s)	Composition	Axial strain of coal sample (10^{-3})	Radial strain of coal sample (10^{-3})	Axial strain of rock sample (10^{-3})	Radial strain of rock sample (10^{-3})
0.002	Coal sample	13.02	4.51	-	-
	Rock sample	-	-	7.33	1.63
	R2C3	10.73	3.12	2.21	0.41
	R1C1	9.89	2.94	2.43	0.36
	R3C2	9.03	2.86	2.82	0.33
0.004	Coal sample	11.21	3.43	-	-
	Rock sample	-	-	7.77	1.55
	R2C3	10.36	3.23	2.12	0.39
	R1C1	9.71	3.06	2.32	0.35
	R3C2	8.87	3.12	2.56	0.34
0.006	Coal sample	11.49	3.41	-	-
	Rock sample	-	-	8.63	1.41
	R2C3	10.21	3.35	1.97	0.37
	R1C1	9.60	3.02	2.04	0.31
	R3C2	8.33	3.09	2.25	0.33

found by the following equation:

$$\varepsilon_{rm} = \frac{\Delta h_{rm}}{h_{rm}}, \ \varepsilon_r = \frac{\Delta h_r}{h_r}, \ \varepsilon_m = \frac{\Delta h_m}{h_m}, \tag{2}$$

where ε_{rm}, ε_r and ε_m are the axial strains of the combination, rock, and coal, separately, while h_{rm}, h_r and h_m are the heights of the combination, rock, and coal, separately.

Given that the strength of the rock specimens developed in this study were close to those of the coal samples (the strengths of the rock samples were 2.3 − 2.6 times those of the coal specimens), during the loading process, rapid crack propagation in the coal specimen released many energies, lead to plastic damage and distortion of the rock sample Liu et al. (2014). At the same time, the two materials above and below the assembly underwent nonuniform deformation. Therefore, the values of ε_{rm}, ε_r and ε_m could be obtained by the testing machine and the strain monitoring system combined with Eq. (2). When uniaxial loading reached the peak load, the central axial and radial strains of the individual specimens and CRC samples are shown in Table 2, the average of the two specimens was taken as the strain.

By analyzing the strain value of the sample under peak load in Table 2, we could obtain the following: The axial and radial strains of the rock samples in the CRC were lesser than the coal samples. The radial strain of the combined coal specimen was less than that of the single coal specimen, which is due to the great strength and strong resistance to distortion of the upper rock sample. The presence of the rock sample had a ring influence on the coal-rock interface and the lower coal sample, which could effectively inhibit the radial strain of the coal specimen. Instead, the distortion of the coal specimen was limited, and some of the energy was transferred from the coal-rock interface to the rock specimen, resulting in the distortion of the rock specimen. The coal-rock height ratio also affected the deformation of the CRC. As the proportion of the rock sample augmented, the axial deformation of the coal sample showed an obvious decreasing trend, and the decreasing trend in radial deformation was not obvious. For the coal specimen under disparate loading speeds, the radial deformations fluctuated.

4.3 Evolution Properties of AE

4.3.1 AE Evolution Properties of Individual Coal and Rock Samples

The AE signal corresponds to the microfracture or damage event inside the sample, so the AE count reflected the number of microfractures and the damage evolution inside the sample. Fig. 12 shows that according to the accumulated AE event counts, the AE activity of the sample could be divided into three stages: the quiet period, the transition period and the active period.

As shown in Fig. 12, there were relatively few AE events in both the quiet period and the transitional period. In view of the soften by straining of coal samples after the peak and the obvious brittle failure and short-term residual strength of rock samples, the active periods of the two were different. After the former reached the peak strength, it entered the post-peak damage stage. The internal structure of the specimen constantly adjusted under the action of loading. The stress dropped slightly at first, and then more slowly, and after a sustained period, the stress dropped sharply, and the bearing capacity of the sample completely failed. During this process, the AE underwent a process of surge-decrease-stabilization-surge: The AE event increases sharply in position corresponding to the stress drop immediately after. Meanwhile, macro-scale cracks were observed in the sample during the surge of AE, and overall damage occurred during the final increase. The latter produced many AE events at the moment of brittle failure. In the residual strength stage, the bearing

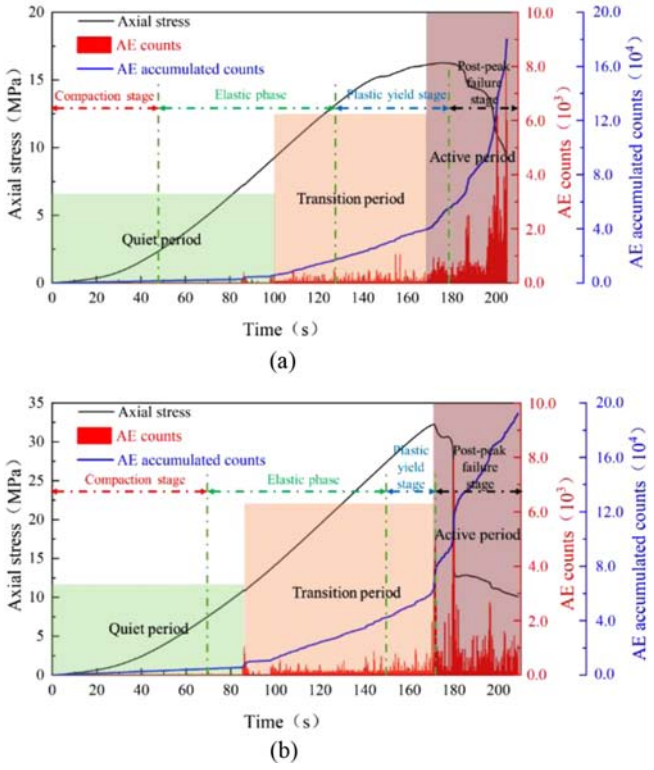

Fig. 12. Evolution of AE Events during the Loading Process: (a) C-6-1, (b) R-6-1

capacity of the sample was mainly provided by the bite force between the broken blocks of the sample and the friction force on the fracture surface. The continuous adjustment was accompanied by crack development and sprouting of new cracks. In addition, sliding friction occurred on the fracture surface, resulting in more active AE activities.

4.3.2 AE Evolution Characteristics of CRC Specimens

Taking the ratio of rock-coal height equal to 1:1 as an example, the evolution behavior of AE events in the loading process of some R1C1 series specimens are given, which is a convenient method to study the AE properties of CRC under disparate loading rates.

In Fig. 13, the AE activities of the CRC samples underwent three stages: calm period, transitional period and active period. The evolution of amount AE events of the CRC specimens under disparate loading rates was obtained: The plastic distortion stage of the CRC sample became shorter with increasing loading rate, while the proportion of the quiet period increased. Additionally, the transition and active periods became shorter as well. AE events were concentrated before and after the time when the samples were obviously brittle due to the relatively short force action time, resulting in an accumulation of fewer AE events. It was the reason why the σ-ε curves in the Fig. 13(c) were smooth without fluctuation. When the loading rate was slow, the internal microcracks of the CRC sample were fully expanding, the plastic deformation stage was relatively long, the time ratio between the

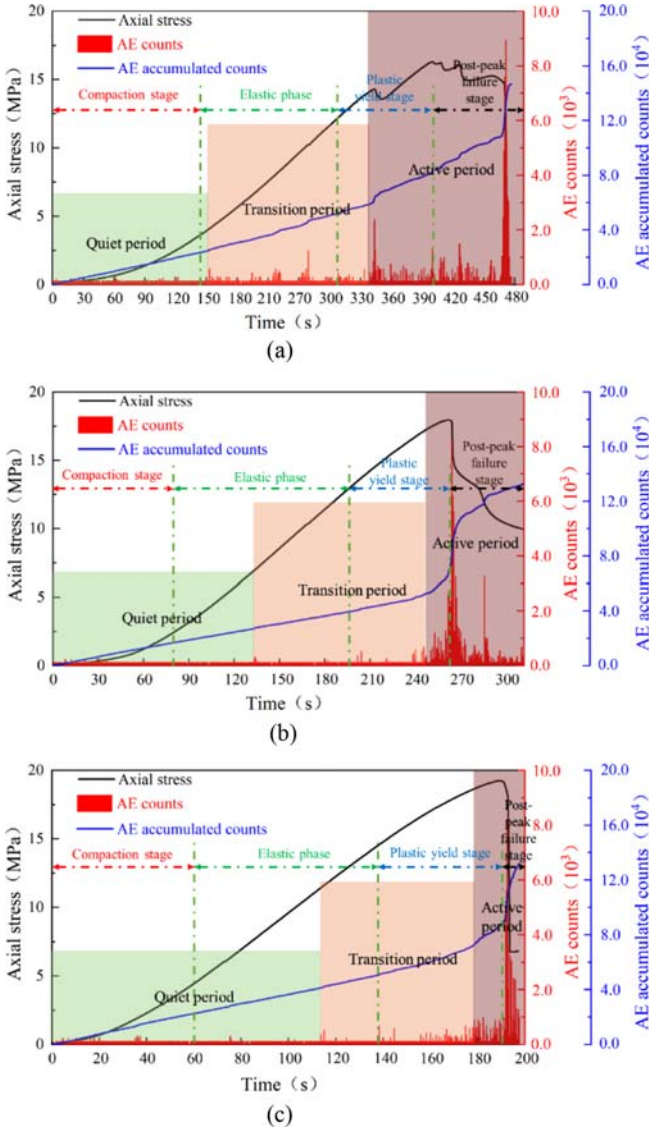

Fig. 13. Evolution of AE Events during Loading of CRC Samples with Coal-Rock Height Ratio of 1:1: (a) R1C1-2, (b) R1C1-4, (c) R1C1-6

transition period and the active period increased significantly, the distribution range of AE events was relatively wide, and the moment of overall failure of the sample was still during the peak period of the AE event. Because the axial force action time was relatively longer than that of the sample with a large loading rate, the cumulative count of the AE event was relatively large.

For instance, the loading rate is 0.002 mm/s, the evolution behavior of AE events in the loading process of CRC with disparate rock-coal height ratios is given, which is convenient for studying the effect of rock-coal height ratio on AE characteristics of CRC. Fig. 14 shows ratio of coal to rock height had few influences on the value of the single AE event count peak but had some influence on the cumulative AE event count. When the height of the coal rock was relatively small, the proportion of the coal specimen in the CRC was larger, the proportion of the relatively hard rock sample part is smaller, the proportion of the

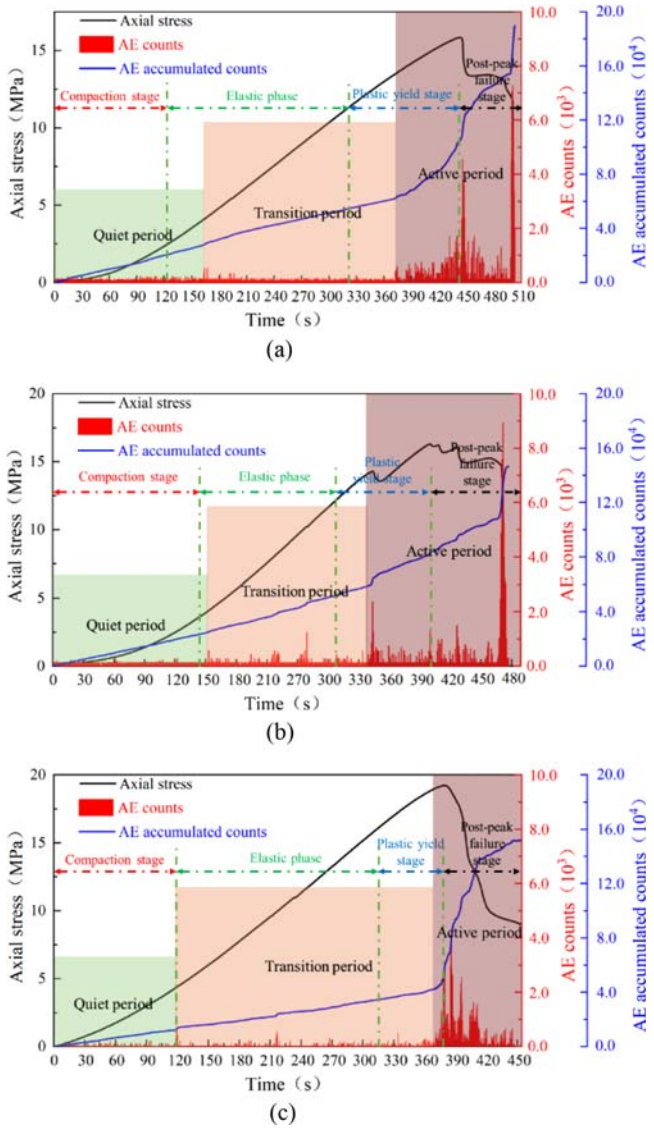

Fig. 14. AE Event Evolution of CRC Samples with the Same Loading Rate and Different Rock Coal Height Ratios: (a) R2C3-2, (b) R1C1-2, (c) R3C2-2

part prone to fracture in the CRC sample increased, and the proportion of the rock sample was small. The suppression effect on the partial deformation of the coal specimen was minor, resulting in a grow in the cumulative AE event count. In contrast, the proportion of relatively hard rock samples in the CRC sample increased, and the rock sample had a certain restrictive effect on the distortion of the coal sample. Therefore, the cumulative AE event counts were fewer compared to samples with small rock-coal height.

4.4 Failure Mode

4.4.1 Damage Patterns of Individual Coal and Rock Specimens

The damage patterns of individual coal and rock specimens with equal strength were approximately the same under different loading rates, and tensile damage was the main damage pattern. The specific failure modes were listed in Table 3.

Table 3 shows that the coal sample was mainly damaged by tension. Significant strain concentration and deformation localization where cracks develop more rapidly. With increasing loading rate, the damage degree was aggravated and accompanied by spalling. The individual rock sample was also dominated by tensile failure; fracture failure changed to tensile failure with increasing loading rate. The rock was also spalled, and the formation process of spalling could be influenced by the number of flaws.

4.4.2 Damage Patterns of CRC

Under disparate height ratios and loading rates, shear and tension-tension coupled damage was the main damage pattern of CRC sample. The coal sample was the main bearing body of CRC structure, and the damage mode of the coal sample determined the coupled failure mode, as shown in Table 4.

Table 4 shows that the damage of the CRC specimen started at the coal-rock interface, and the cracking began in the coal sample. The loading of the coal sample accumulated many elastic deformation energies, some of which was used for self-deformation,

Table 3. Failure Modes of Individual Samples with Equal Strength of Coal and Rock

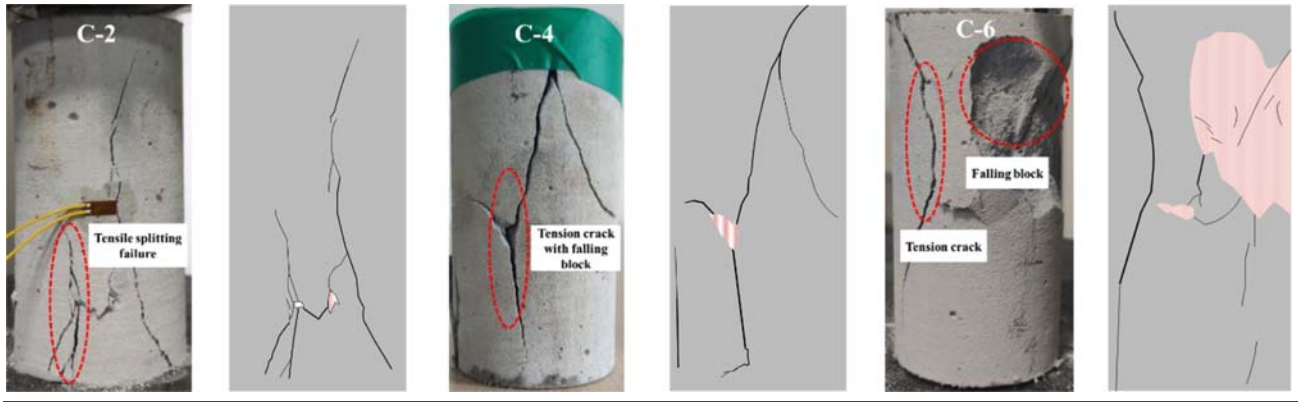

Loading rate 0.002 mm/s	Loading rate 0.004 mm/s	Loading rate 0.006 mm/s

Table 3. (continued)

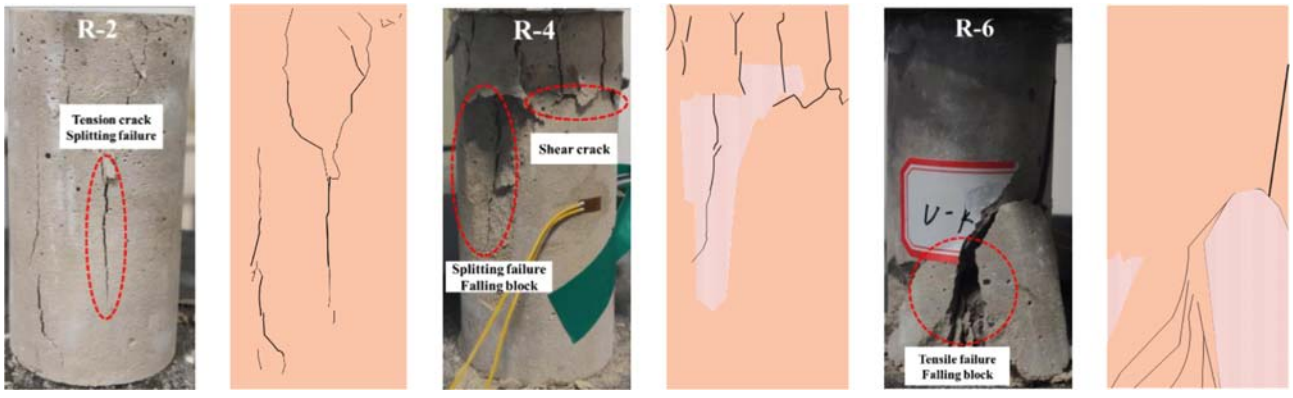

Loading rate 0.002 mm/s | Loading rate 0.004 mm/s | Loading rate 0.006 mm/s

and some of which was transferred to the rock sample, resulting in cracks in the rock sample. As the coal-rock height ratio increases, the coal sample was the main body bearing the load and undergoing deformation failure, but the degree of deformation and damage of the rock sample gradually reduced. When the height ratio was 2:3, the coupled damage mode of the CRC was tensile failure. When the height ratio was 1:1 or 3:2, the CRC sample was dominated by the shear-coupled failure mode. When loading rate of 0.006 mm/s, the coupled failure way of the CRC sample showed obvious characteristics of shear failure.

5. Conclusions

This study focused on investigating coal-like and rock-like

Table 4. Coupled Failure Modes of CRC Samples

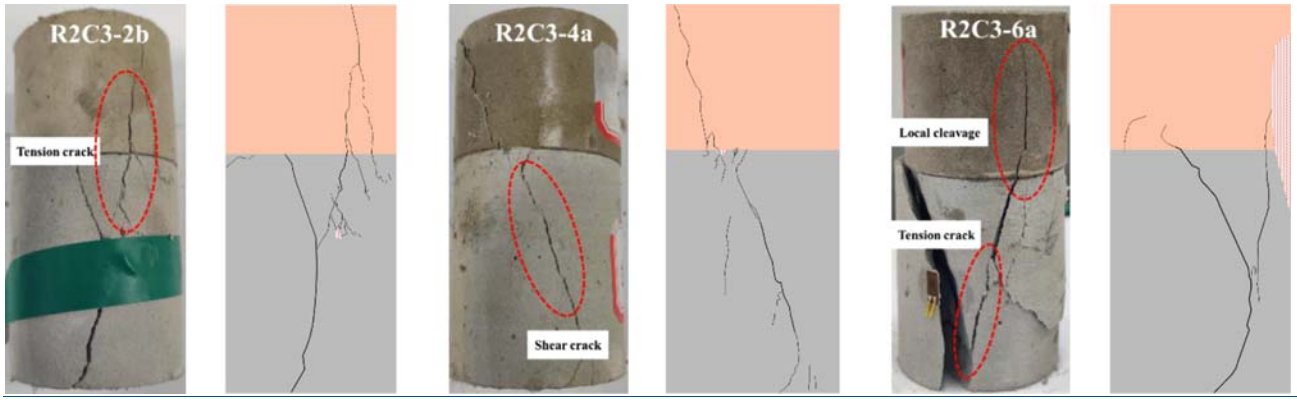

Height ratio 2:3 | Height ratio 2:3 | Height ratio 2:3

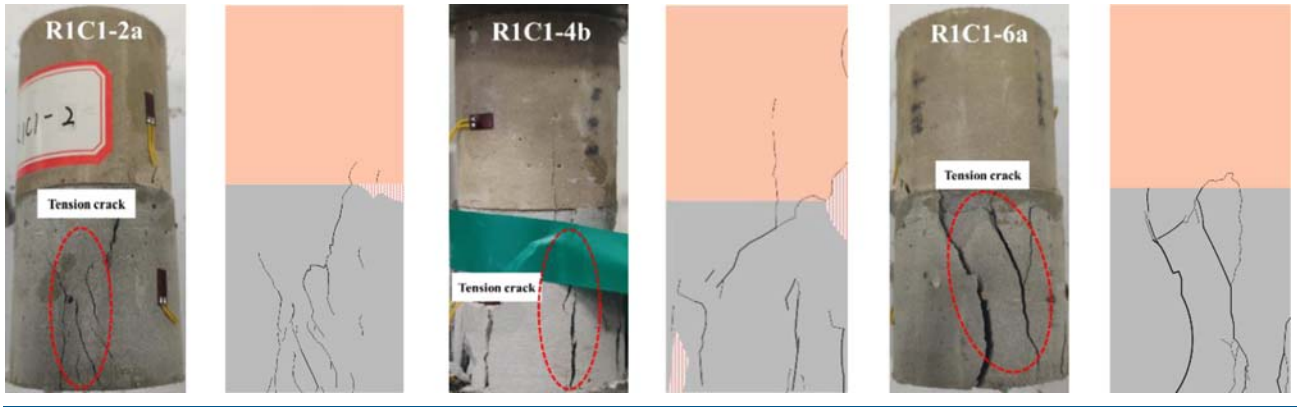

Height ratio 1:1 | Height ratio 1:1 | Height ratio 1:1

Table 4. (continued)

 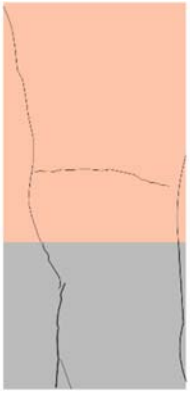	 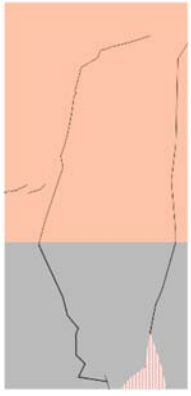	 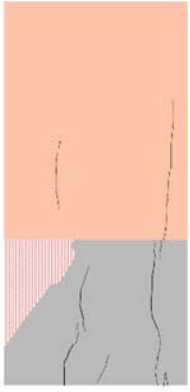
Height ratio 3:2	Height ratio 3:2	Height ratio 3:2

samples and CRC samples that were developed and processed using materials with equal strength are taken as the research objects. Using an electronic universal testing machine, a static strain testing system and an AE monitoring system, UC tests were conducted for CRC with equal strength for disparate rock-coal height ratios and loading rates. By analyzing the strength, deformation and AE properties of the CRC samples, and studying the coupled damage mode of the CRC sample, the following findings were obtained:

1. The damage modes of individual coal and rock samples with equal strength were mainly tensile failure, and the σ-ε curves included four stages: compaction, elastic distortion, plastic yield and post-peak damage. The compaction stage of individual samples with equal strength of coal was more obvious, while the brittle failure of individual samples with equal strength of rock was more obvious after the peak. The peak intensities of the coal and rock specimens increased with increasing loading rate. The strengths of the rock samples increased approximately linearly, while those of the coal samples increased nonlinearly. The E of the coal and rock with equal strength samples increased to various degrees with increasing loading rate, while μ decreased to various degrees.
2. The AE characteristics of individual coal and rock specimens and CRC specimens, all with equal strengths, differed. The active stages of AE activities of signal coal and rock specimens were in the plastic stage and the post-peak stage. During the periods before and after the stress peak are when the AE event count reached the maximum value. However, the single counting peak values of the AE event of the CRC samples were not greatly influenced on the rock-coal height ratio, although the number of cumulative AE events was affected to a certain extent, and the loading rate had a strong effect on the AE properties of the CRC.
3. The damage modes of CRC samples were disparate those of individual samples: When the rock-coal height ratio is 2:3, the failure mode was guided by tensile damage; when the height ratio was 1:1 and 3:2, the damage mode was alternately tensile-shear damage and tensile failure, and when loading rate is 0.006 mm/s, the coupled failure mode of CRC samples showed obvious characteristics of shear failure. As the loading rate increases, the compaction stage and elastic deformation stage of the CRC samples were significantly shorter, and the post-peak brittle damage of the samples was more obvious. When the height ratio was small, the σ-ε curve was smooth. When the height ratio increased, the curve fluctuated in the pre-peak stage. The E and strength of the CRC samples increased with increasing coal-rock height ratio and loading rate.

Acknowledgments

This work was supported by the China Postdoctoral Science Foundation (No. 2023M732109), the Shandong Postdoctoral Science Foundation (No. SDCX-ZG-202303031), the Opening Foundation of Shandong Key Laboratory of Civil Engineering Disaster Prevention and Mitigation (No. CDPM2021FK02) and the Youth Innovation Team of Shandong Higher Education Institutions (No. 2022KJ214). We would like to acknowledge the editor and reviewers for their valuable comments, which have greatly improved this paper.

ORCID

Maolin Tian https://orcid.org/0000-0003-2429-1597

References

Abi E, Yuan H, Cong Y, Wang Z, Jiang M (2023) Experimental study on the entropy change failure precursors of marble under different stress paths. *KSCE Journal of Civil Engineering* 27(1):356-370, DOI: 10.1007/s12205-022-1975-3

Ali M, Wang E, Li Z, Wang X, Khan NM, Zang Z, Alarifi SS, Fissha Y (2023) Analytical damage model for predicting coal failure stresses by utilizing acoustic emission. *Sustainability* 15(2):1236, DOI: 10.3390/

su15021236

Bai JW, Feng GR, Wang ZH, Wang SY, Qi TY, Wang PF (2019) Experimental investigations on the progressive failure characteristics of a sandwiched coal-rock system under uniaxial compression. *Applied Sciences* 9(6):1195, DOI: 10.3390/app9061195

Chakraborty S, Bisai R, Palaniappan SK, Pal SK (2019) Failure modes of rocks under uniaxial compression tests: An experimental approach. *Journal of Advances in Geotechnical Engineering* 2(3):1-8, DOI: 10.5281/zenodo.3461773

Chen SJ, Yin DW, Jiang N, Wang F, Guo WJ (2019) Simulation study on effects of loading rate on uniaxial compression failure of composite rock-coal layer. *Geomechanics and Engineering* 17(4):333-342, DOI: 10.12989/GAE.2019.17.4.333

Chen Y, Zuo JP, Song HQ, Feng LL, Shao GY (2018) Deformation and crack evolution of coal-rock combined body under cyclic loading-unloading effects. *Journal of Mining & Safety Engineering* 35(4):826-833, DOI: 10.13545/j.cnki.jmse.2018.04.022

Choi S, Jeong H, Cheon DS (2022) Prediction of mohr-coulomb constants of selected korean rocks based on extreme gradient boosting method and its evaluation. *KSCE Journal of Civil Engineering* 26(5):2468-2477, DOI: 10.1007/s12205-022-1388-3

Dambly MLT, Nejati M, Vogler D, Saar MO (2019) On the direct measurement of shear moduli in transversely isotropic rocks using the uniaxial compression test. *International Journal of Rock Mechanics and Mining Sciences* 113:220-240, DOI: 10.1016/j.ijrmms.2018.10.025

Das AJ, Paul PS, Mandal PK, Kumar R, Tewari S (2021) Investigation of failure mechanism of inclined coal pillars: Numerical modelling and tensorial statistical analysis with field validations. *Rock Mechanics and Rock Engineering* 54(6):3263-3289, DOI: 10.1007/s00603-021-02456-5

Fan Y, Chen J, Leng ZD, Yang GD, Liu XF, Tian B (2024a) Punching mechanism of air-deck stemming for drilling blasting and its influence on rock fragmentation. *Rock Mechanics and Rock*, DOI: 10.1007/s00603-024-03773-1

Fan Y, Yang GD, Cui XZ, Zhao XH, Wu JG, Wang LH (2024b) Low-frequency characteristics of vibrations induced by transient unloading of in situ stress and its influence on safety of a deeply buried tunnel. *International Journal of Geomechanics*, DOI: 10.1061/IJGNAI.GMENG-8190

Gao FQ, Kang HP, Yang L (2020) Experimental and numerical investigations on the failure processes and mechanisms of composite coal-rock specimens. *Scientific Reports* 10(1):13422, DOI: 10.1038/s41598-020-70411-5

Gong FQ, Ye H, Luo Y (2018) The effect of high loading rate on the behaviour and mechanical properties of coal-rock combined body. *Shock and Vibration* 2018:1-9, DOI: 10.1155/2018/4374530

Khazaei C, Hazzard J, Chalaturnyk R (2015) Damage quantification of intact rocks using acoustic emission energies recorded during uniaxial compression test and discrete element modeling. *Computers and Geotechnics* 67:94-102, DOI: 10.1016/j.compgeo.2015.02.012

Li XL, Chen SJ, Wang EY, Li ZH (2021) Corrigendum to "Rockburst mechanism in coal rock with structural surface and the microseismic (MS) and electromagnetic radiation (EMR) response" [Eng. Fail. Anal. 124 (2021) 105396]. *Engineering Failure Analysis* 128:105523, DOI: 10.1016/j.engfailanal.2021.105523

Li CJ, Xu Y, Ye ZY (2020) Energy dissipation and crushing characteristics of coal-rock-like combined body under impact loading. *Chinese Journal of Geotechnical Engineering* 42(5):981-988, DOI: 10.11779/CJGE202005022

Li FX, Yin DW, Wang F, Jiang N, Li XL (2022) Effects of combination mode on mechanical properties of bi-material samples consisting of rock and coal. *Journal of Materials Research and Technology* 19:2156-2170, DOI: 10.1016/j.jmrt.2022.05.174

Liu XS, Tan YL, Ning JG, Lu YW, Gu QH (2018) Mechanical properties and damage constitutive model of coal in coal-rock combined body. *International Journal of Rock Mechanics and Mining Sciences* 110:140-150, DOI: 10.1016/j.ijrmms.2018.07.020

Liu J, Wang EY, Song DZ, Yang SL, Niu Y (2014) Effects of rock strength on mechanical behavior and acoustic emission characteristics of samples composed of coal and rock. *Journal of China Coal Society* 39(4):685-691, DOI: 10.13225/j.cnki.jccs.2013.1490

Ma SZ, Liu KW, Guo TF, Yang JC, Li XD, Yan ZX (2022a) Experimental and numerical investigation on the mechanical characteristics and failure mechanism of cracked coal & rock-like combined sample under uniaxial compression. *Theoretical and Applied Fracture Mechanics* 122:103583, DOI: 10.1016/j.tafmec.2022.103583

Ma SZ, Lu KW, Guo TF, Huang XH, Zhou ZX (2022b) Numerical analysis of dynamic mechanical characteristics of brazilian splitting of coal-rock combination bodies. *Chinese Journal of High Pressure Physics* 36(5):128-140, DOI: 10.11858/gywlxb.20220589

Ma Q, Tan YL, Liu XS, Zhao ZH, Fan DY, Purev L (2021) Experimental and numerical simulation of loading rate effects on failure and strain energy characteristics of coal-rock composite samples. *Journal of Central South University* 28(10):3207-3222, DOI: 10.1007/s11771-021-4831-6

Okubo S, Fukui K, Qing XQ (2006) Uniaxial compression and tension tests of anthracite and loading rate dependence of peak strength. *International Journal of Coal Geology* 68(3-4):196-204, DOI: 10.1016/j.coal.2006.02.004

Shadrin A, Klishin V (2018) Acoustic emission of rock mass under the constant-rate fluid injection: IOP Conference Series. *Earth and Environmental Science* 134:012057, DOI: 10.1088/1755-1315/134/1/012057

Tan Y, Liu XS, Ning JG, Lu YW (2017) In situ investigations on failure evolution of overlying strata induced by mining multiple coal seams. *Geotechnical Testing Journal* 40(2):20160090, DOI: 10.1520/GTJ20160090

Tan YL, Liu XS, Shen B, Ning JG, Gu QH (2018) New approaches to testing and evaluating the impact capability of coal seam with hard roof and/or floor in coal mines. *Geomechanics and Engineering* 14(4):367-376, DOI: 10.12989/GAE.2018.14.4.367

Wang P, Jia HJ, Zheng PQ (2020a) Sensitivity analysis of bursting liability for different coal-rock combinations based on their inhomogeneous characteristics. *Geomatics Natural Hazards and Risk* 11:149-159, DOI: 10.1080/19475705.2020.1714754

Wang T, Ma Z (2022) Research on strain softening constitutive model of coal-rock combined body with damage threshold. *International Journal of Damage Mechanics* 31(1):22-42, DOI: 10.1177/10567895211019068

Wang T, Ma ZG, Gong P, Li N, Cheng SX (2020b) Analysis of failure characteristics and strength criterion of coal-rock combined body with different height ratios. *Advances in Civil Engineering* 2020:1-14, DOI: 10.1155/2020/8842206

Wang T, Qi FZ, Chang JC (2022a) Analysis of energy transmission and deformation characteristics of coal-rock combined bodies. *Geofluids* 2022:1-11, DOI: 10.1155/2022/5304250

Wang X, Tian LG (2018) Mechanical and crack evolution characteristics of coal-rock under different fracture-hole conditions: A numerical study based on particle flow code. *Environmental Earth Sciences* 77(8):297, DOI: 10.1007/s12665-018-7486-3

Wang TN, Zhai Y, Gao H, Li YB, Li Y, Sun WZ, Yan TY (2022b) A

macroscopic elastic model of coal-rock combined body under static compression before cracking. *Rock and Soil Mechanics* 43(4):1031-1040, DOI: 10.16285/j.rsm.2021.1075

Xia ZG, Liu S, Bian Z, Song JH, Feng F, Jiang N (2021) Mechanical properties and damage characteristics of coal-rock combination with different dip angles. *KSCE Journal of Civil Engineering* 25(5): 1687-1699, DOI: 10.1007/s12205-021-1366-1

Xiong Y, Yang SL, Kong DZ, Song GF, Ma ZQ, Zuo YJ (2023) Analysis on early warning of coal sample failure based on crack development law and strain evolution characteristics. *Engineering Failure Analysis* 148:107170, DOI: 10.1016/j.engfailanal.2023.107170

Xu J, Ma L, Xiao XC, Wu D (2023) Experimental study of the formation process and behaviors of spalling in rock materials. *Engineering Failure Analysis* 143:106873, DOI: 10.1016/j.engfailanal.2022.106873

Yang Z, Li Y, Li X, Zhuang JY, Li H, Wang X, Wang YN, Du F (2021) Multifield coupling mechanism of unloading deformation and fracture of composite coal-rock. *Shock and Vibration* 2021:1-16, DOI: 10.1155/2021/2450330

Yang EH, Li SG, Lin HF, Zhao PX, Qin L, Zhao B (2022) Influence mechanism of coal thickness effect on strength and failure mode of coal-rock combination under uniaxial compression. *Environmental Earth Sciences* 81(17):429, DOI: 10.1007/s12665-022-10533-3

Yang K, Wei Z, Chi XL, Zhang YG, Dou LT, Liu WJ (2020) Experimental research on the mechanical characteristics and the failure mechanism of coal-rock composite under uniaxial load. *Advances in Civil Engineering* 2020:1-11, DOI: 10.1155/2020/8867809

Yin DW, Chen SJ, Ge Y, Liu R (2021) Mechanical properties of rock-coal bi-material samples with different lithologies under uniaxial loading. *Journal of Materials Research and Technology* 10:322-338, DOI: 10.1016/j.jmrt.2020.12.010

Yin DW, Chen SJ, Liu XQ, Ma HF (2018) Effect of joint angle in coal on failure mechanical behaviour of roof rock-coal combined body. *Quarterly Journal of Engineering Geology and Hydrogeology* 51(2):202-209, DOI: 10.1144/qjegh2017-041

Závacký M, Štefaňák J (2019) Strains of rock during uniaxial compression tests. *Stavební obzor - Civil Engineering Journal* 28(3), DOI: 10.14311/CEJ.2019.03.0032

Zhang H (2019) Study on the influence of local impact on coal-rock microstructures and equivalent theoretical model. MSc Thesis, China University of Mining Technology, Beijing, China (in Chinese)

Zhang CL, Dong Y, Feng RM, Peng NB, Zhang JH, Wu JK, Shen W, Du F (2021) Crack propagation law and failure characteristics of coal-rock combined body with the different inclination angle of prefabricated fissure. *Geofluids* 2021:1-13, DOI: 10.1155/2021/4348912

Zhang H, Lu CP, Liu B, Liu Y, Zhang N, Wang HY (2020) Numerical investigation on crack development and energy evolution of stressed coal-rock combination. *International Journal of Rock Mechanics and Mining Sciences* 133:104417, DOI: 10.1016/j.ijrmms.2020.104417

Zhao TB, Gu XB, Guo WY, Gong XF, Xiao YX, Kong B, Zhang CG (2021) Influence of rock strength on the mechanical behavior and P-velocity evolution of coal-rock combination specimen. *Journal of Materials Research and Technology* 12:1113-1124, DOI: 10.1016/j.jmrt.2021.03.059